


Empirics of multimodal traffic networks - Using the 3D macroscopic fundamental diagram

Working Paper**Author(s):**

Loder, Allister; Ambühl, Lukas; Menendez, Monica; Axhausen, Kay W. 

Publication date:

2016-12

Permanent link:

<https://doi.org/10.3929/ethz-b-000124043>

Rights / license:

In Copyright - Non-Commercial Use Permitted

Originally published in:

Arbeitsberichte Verkehrs- und Raumplanung 1225

Empirics of multimodal traffic networks - Using the 3D macroscopic fundamental diagram

Allister Loder

Lukas Ambühl

Monica Menendez

Kay W. Axhausen

Working paper

Institute for Transport Planning and Systems

1225

December 2016

Working paper

1225

Empirics of multimodal traffic networks - Using the 3D macroscopic fundamental diagram

Allister Loder
IVT
ETH Zürich

CH-8093 Zürich
phone: +41-44-633 62 58
fax: +41-44-633 10 57
allister.loder@ivt.baug.ethz.ch

Monica Menendez
IVT
ETH Zürich

CH-8093 Zürich
phone: +41-44-633 66 95
fax: +41-44-633 10 57
monica.menendez@ivt.baug.ethz.ch

Lukas Ambühl
IVT
ETH Zürich

CH-8093 Zürich
phone: +41-44-633 32 51
fax: +41-44-633 10 57
lukas.ambuehl@ivt.baug.ethz.ch

Kay W. Axhausen
IVT
ETH Zürich

CH-8093 Zürich
phone: +41-44-633 39 43
fax: +41-44-633 10 57
axhausen@ivt.baug.ethz.ch

December 2016

Abstract

Traffic is multimodal in most cities. However, the impacts of different transport modes on traffic performance and on each other, are unclear – especially at the network level. The recent extension of the macroscopic fundamental diagram (MFD) to the 3D-MFD, offers a novel framework to address this gap at the urban scale. The 3D-MFD relates the network density of cars and public transport vehicles to the network flow, for either vehicles or passengers. No empirical 3D-MFD has been reported so far.

In this paper, we present the first empirical estimate of a 3D-MFD at the urban scale. To this end, we use data from loop detectors and automatic vehicle location devices (AVL) of the public transport vehicles in the city of Zurich, Switzerland. We compare two different areas within the city, that differ in their topology and share of dedicated lanes to public transport. We propose a statistical model of the 3D-MFD, which estimates the effects of the demands on car and public transport speeds. The results quantify the multimodal effects of both, vehicles and passengers, and confirms that a greater share of dedicated lanes reduces the marginal effect of public transport vehicles on car speeds. Lastly, we derive a new application of the 3D-MFD, by identifying the share of public transport users that maximizes the journey speeds in an urban network accounting for all motorized transport modes.

Preferred citation style

Loder, A., L. Ambühl, M. Menendez and K. W. Axhausen (2016) Empirics of multimodal traffic networks - Using the 3D macroscopic fundamental diagram, *Working paper*, **1225**, Institute for Transport Planning and Systems (IVT), ETH Zurich, Zurich.

1 Introduction and background

Potential benefits from public transport provision and improvements in urban transportation networks are not limited to reduction in passengers' travel time (Hensher, 2001) or congestion relief (Adler and van Ommeren, 2016; Anderson, 2014), but also include an increase in agglomeration economies (Chatman and Noland, 2011). Identifying that optimal share of public transport users (from a set of all users) to maximize these benefits is abundantly documented in literature (Small and Verhoef, 2007; Tirachini and Hensher, 2012). While infrastructure investments for both modes are long-term-oriented, an optimal modal share of public transport users for the short term considers how travel demand should be allocated to existing infrastructure while improving accessibility for all users. Recent advances in understanding network-wide traffic through the macroscopic fundamental diagram (MFD), a well-defined and reproducible relationship between vehicle network accumulation and network flow (Geroliminis and Daganzo, 2008), offer a new approach for optimal demand allocation to existing infrastructure. The MFD is considered invariant to small changes in demand and network topology determines its shape (Daganzo and Geroliminis, 2008). Public transport and private cars do not affect congestion equally (Boyac and Geroliminis, 2011; Chiabaut et al., 2016; Gronau, 2000). To properly account for these two systems, the MFD must be extended to the bimodal or 3D-MFD (Geroliminis et al., 2014) that integrates transport modes. Although promising, no empirical 3D-MFD has yet been found. Such empirical study, however, is crucial for further applications of the 3D-MFD in transportation and economics.

In this paper, we present the first empirical estimate of a 3D-MFD the urban scale, using data from loop detectors and automatic vehicle location devices (AVL) for the city of Zurich, Switzerland. We combine both vehicle and passenger data to econometrically estimate the bi-modal interaction costs at vehicle and passenger levels. We compare interaction costs for two regions in the city of Zurich differing in their share of dedicated lanes. We find evidence that cars and public transport vehicles do not contribute equally to congestion and that a greater share of dedicated lanes reduces bi-modal interaction costs. Finally, we derive a new application of the 3D-MFD, by linking the share of public transport users and average journey speeds in the city. Using this approach, we then identify an optimal share of public transport users to maximize journey speeds in an urban area (considering all motorized transport modes).

In the following, we give a literature overview. First, we concentrate on the car MFD, then on interactions between cars and public transport at a network level, from both vehicle and passenger perspectives, including the concept of the 3D-MFD.

Origins of the MFD can be traced back to network traffic flow theory in the 1960s and are

based on work by Smeed (1961, 1968), Thomson (1967), Wardrop (1968) and Godfrey (1969). In the 1980s, Mahmassani et al. (1984, 1987) and Williams et al. (1987) used simulations to relate average speed, flow and density at the network level. The studies found that the network relationships of these variables are similar to their link-based counterparts. Daganzo and Geroliminis (2008) used variational theory to analytically derive the MFD as a characteristic of a network (free flow speed, average link length, link capacity, traffic signal cycle characteristics, jam density and backward wave speed) and found it to be a well-defined, reproducible and concavely curved. In addition to simulation and analytical estimates of the MFD, the macroscopic relationship has also been observed with empirical data. The MFD has been shown to exist for Yokohama, Japan (Geroliminis and Daganzo, 2008), Toulouse, France (Buisson and Ladier, 2009), Brisbane, Australia (Tsubota et al., 2014), Shenzhen, China (Ji et al., 2014), Sendai, Japan (Wang et al., 2015) and Zurich, Switzerland (Ambühl et al., 2017). Such estimates are typically based on either loop detector data (LDD) or floating car data (FCD), although both data sources have drawbacks. The spatial distribution of loop detectors within the link and network affects the shape of the MFD significantly (Buisson and Ladier, 2009; Ambühl et al., 2017). An MFD based on FCD, on the other hand, is sensitive to an inhomogeneous distribution of probe vehicles across the network (Du et al., 2016), and to the fact that probe vehicles might not be a representative sample of the entire vehicle fleet, e.g. taxis (Geroliminis and Daganzo, 2008; Ji et al., 2014). Recent efforts aim to overcome limitations of both data sources, e.g. by using fusion algorithms (Ambühl and Menendez, 2016) or combining data sources (Courbon and Leclercq, 2011; Ambühl et al., 2017).

The MFD was applied to traffic control (e.g. Haddad and Geroliminis (2012); Aboudolas and Geroliminis (2013)), pricing (Zheng et al., 2012, 2016), investigation of network topology's impact on traffic performance (Knoop et al., 2014, 2015; Ortigosa et al., 2015; Muhlich et al., 2015) and to describe the effects of other systems, in particular parking (Geroliminis, 2015; Zheng and Geroliminis, 2016a; Cao and Menendez, 2015).

Although public transport plays an important role in cities, its impact on traffic at the network level has not received much attention in literature. At the link level, analytical approaches have been developed to quantify maximum capacity of mixed traffic and analyze the effects of stop types, dwell times and distance between stops on speeds (Köhler et al., 1998; Anderhub et al., 2008; Chiabaut, 2015; Chiabaut et al., 2016; Lüthy et al., 2016) and empirical data has been used to analyze car capacity with and without busses (Arnet et al., 2015). Additionally, Small and Verhoef (2007) investigated the optimal pricing for both public and private transport modes. At the network level, Smeed (1961, 1968) discussed the effects of car and bus interactions on respective travel times and the effect of urban design on traffic performance, emphasizing the dilemma between public and private transport modes for both travel times and vehicle occupancies. He discussed the relationship between share of car users and average travel time

per kilometer and traveler for a given travel demand in a city. To summarize: the greater the travel demand, the greater the share of public transport users must be to maintain a certain average speed. Work following Smeed's macroscopic relations was almost non-existent for decades, until Boyac and Geroliminis (2011) discussed urban design and multimodal capacities at network level, and Geroliminis et al. (2014) extended the MFD to a 3D-MFD using simulation data. For a network with only mixed traffic lanes, the maximum vehicular flow in a 3D-MFD occurs when no public transport vehicles operate. When including passenger flows, the 3D-MFD becomes the 3D-passenger MFD (3D-pMFD). The maximum passenger flow in a 3D-pMFD, on the other hand, is observed at non-zero provision of public transport. Analogue to the unimodal MFD, Zheng and Geroliminis (2016b) argue that 3D-MFD can be obtained either from analytical approximations or real data. Chiabaut (2015) related the accumulation of passengers per kilometer to passenger flow and discussed the concept of the 3D-MFD for multimodal arterials from a passenger's point of view, emphasizing the user and system optimum. Chiabaut et al. (2016) discuss the design of multimodal arterials with respect to mixed or dedicated lanes. Vasileios et al. (2016) evaluate the impact of different bus network designs on the overall car capacity of the network.

While analytical approximations for MFDs concentrating either on cars (Daganzo and Geroliminis, 2008; Leclercq and Geroliminis, 2013; Geroliminis and Boyacı, 2012) or multimodal MFDs (Boyac and Geroliminis, 2011; Chiabaut, 2015; Chiabaut et al., 2016) exist, empirical MFDs have only been obtained for cars so far. Data describing multimodal relations has been obtained only from simulations of San Francisco and Zurich (Geroliminis et al., 2014; Ortigosa et al., 2017; Menendez et al., 2016).

First applications of the 3D-MFD (and 3D-pMFD) are related to urban space allocation (Zheng and Geroliminis, 2013), parking (Zheng and Geroliminis, 2016a) and mode choice (Schreiber et al., 2016). Further research is suggested to analyze the aggregate performance of both modes with public transport priority (Christofa et al., 2016).

The remainder of this paper is organized as follows; in section 2, we describe the case study for Zurich with the available data. In section 3, we present the empirical 3D-MFD. In section 4, we propose a model to quantify the effects of bi-modal traffic at the network level. In section 5, we show the results of the proposed model for both vehicles and passengers. In section 6, we present a methodology to derive the optimal share of public transport users from the 3D-MFD. We then finish in section 7 with concluding remarks.

Table 1: Statistics of Zurich’s private and public transport network.

		City center	Wiedikon
Car network length, L_c	[lane-km]	39	31
Covered by loop detector	[lane-km]	24	10
Number of signalized intersections		42	22
Public transport network length, L_{pt}	[lane-km]	34	25
Share of lanes dedicated to public transport	[% L_{pt}]	75	60

2 Data

2.1 Analyzed areas and time period

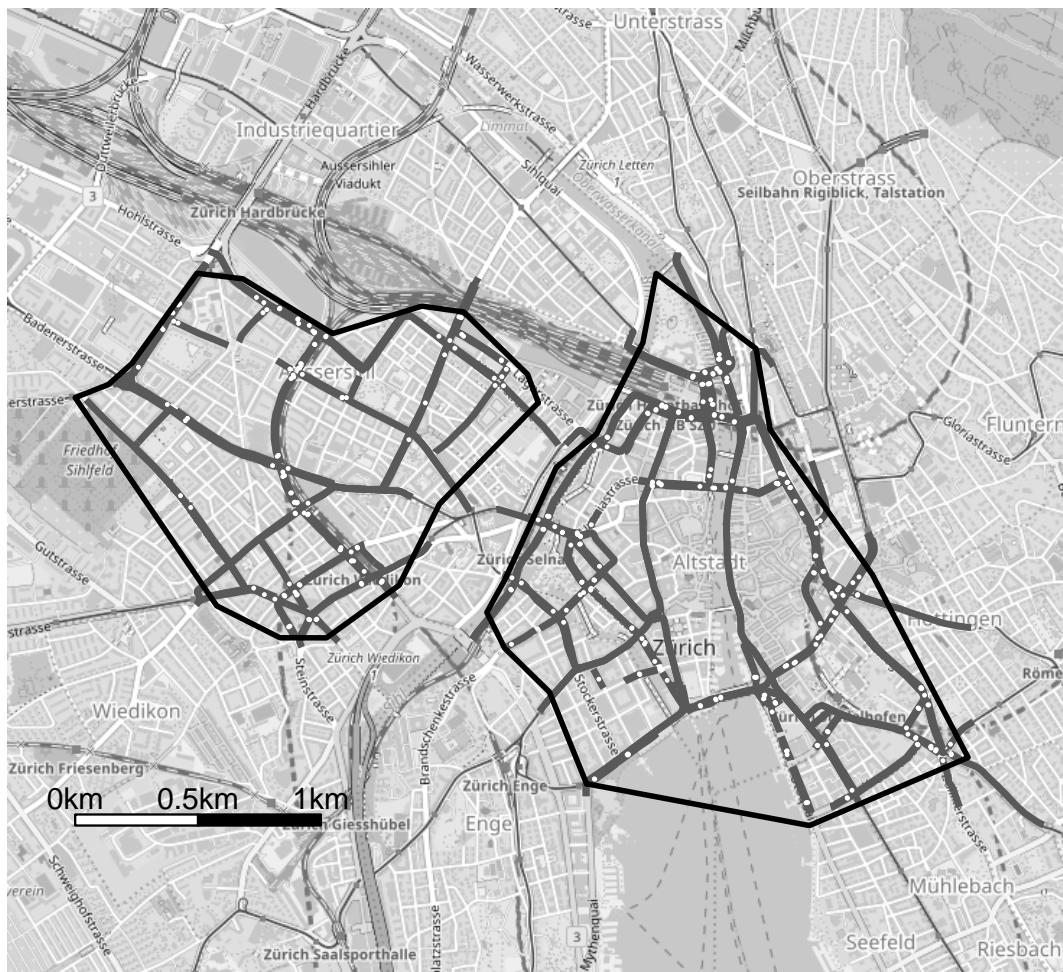
Zurich is the largest city in Switzerland, encompassing an area of around 92 km², with a population of approximately 400’000 and roughly 300’000 daily inbound commuters. The road network, excluding motorways, has a length of 740 km. For the analysis, we concentrate on the time period between the 26th and the 30th of October 2015 (a total of 5 days). For each day, we use data from 06:00 to 24:00 (the public transport operating time). We focus on two regions within Zurich, each with an area of approximately 2 km². Figure 1 shows both regions. We denote the zone in the west as Wiedikon and the zone in the east as City center. The zones are selected for two main reasons. First, both regions differ in their share of public transport dedicated lanes; in the *City center* almost 75 % of the public transport lanes are dedicated, whereas in *Wiedikon* this number is 60 %. Second, we have chosen the area of each region to minimize the likelihood of violating the MFD homogeneity assumption of the MFD (Buisson and Ladier, 2009). Thus, we avoid further partitioning of the network, as in (Ji et al., 2014).

Table 1 summarizes transport network characteristics for both transport modes in the two regions. In the City center, the network length includes 22 km for trams and 12 km for buses, while in Wiedikon, 7 km are for trams and 18 km for busses. Even though both regions have a high share of dedicated lanes for public transport, interactions between both modes occur particularly at intersections and curbside stops.

2.2 Car data

The traffic management system of Zurich operates 4852 traffic detectors at 384 intersections for public transport vehicles, cars, or both (Stadt Zürich - Dienstabteilung Verkehr (DAV), 2015).

Figure 1: Zones of analysis. Map by Map by Open Street Map (2016).



Source: Open Street Map (2016)

Their purpose is to give priority to public transport, support traffic signal control and identify congestion. In this paper, we concentrate on data from loop detectors that measures car traffic. Each detector records vehicle counts, q , and occupancy, o , with a resolution of 0.1 s, aggregated in three minute intervals. Data from malfunctioning loop detectors was removed from the data set. All detectors were geo-coded; then we collected their positions x_i referenced from the next downstream intersection and the link length l_i . Average link length is 220 m. Most detectors are located close to the next downstream intersection and thus, the corresponding traffic density is overestimated (Ambühl et al., 2017; Buisson and Ladier, 2009; Courbon and Leclercq, 2011). In Figure 1, the white dots are the locations of loop detectors and gray lines are the links covered by this analysis. The number of selected loop detectors, N , is 217 in the City center and 114 in Wiedikon.

As density, k , is not directly measured by loop detectors, its value must be approximated by the space-effective mean length, l_e , of a car ($k = o/l_e$). For Zurich, this value is 6.3 m (AKP Verkehrsingenieure AG, 2016; Stadt Zürich - Dienstabteilung Verkehr (DAV), 2015). Ambühl et al. (2017) compared empirical loop detector data with simulation data and developed a correction method that takes loop detectors' spatial distribution into account. For the reader's convenience, from now on we will summarize the approach described in Ambühl et al. (2017). The proposed approach weighs loop detector measurements as if they were uniformly distributed across the length of the links in the entire network. This is required for reliable MFD estimation (Courbon and Leclercq, 2011). In other words, we group loop detectors into J groups defined by their relative position x_i/l_i on link i . Each segment j then holds N_j loop detectors. We then calculate the weighted flow and occupancy of all loop detectors in each segment j . Finally, we take the average flow and occupancy over all segments. After testing for different values of J , we choose $J = 20$, as this value ensures at least one loop detector in each segment. The equations for this correction method for flow, q , and density, k , are given below.

$$\tilde{q}_c = \frac{1}{J} \sum_{j=1}^J \sum_{i \in N_j} \frac{q_i l_i}{\sum l_i} \quad (1)$$

$$\tilde{k}_c = \frac{1}{J_s} \sum_{j=1}^J \sum_{i \in N_j} \frac{o_i l_i}{\sum l_i} \quad (2)$$

$$\text{with } N = \bigcup_{j \in J} N_j \quad \text{and } N_j = \{i \in N \mid \frac{j-1}{J} < \frac{x_i}{l_i} < \frac{j}{J}\}$$

With the corrected \tilde{q}_c and \tilde{k}_c we compute the space-mean speed \tilde{v}_c according to Equation 3.

$$\tilde{v}_c = \frac{\tilde{q}_c}{\tilde{k}_c} \quad (3)$$

Figure 2 shows the resulting MFDs from loop detector data. In Figure 2(a), we observe a higher capacity and critical density in Wiedikon than in the City center. While Wiedikon shows a decrease in flow once critical density is reached, this congested portion of the MFD is absent for the City center. We assume that this is due to Zurich's traffic management scheme. For the City center, a gating control operates, designed to reduce congestion during peak hours. Thus, we do not expect strong indications of congestion. Additionally, the reduced capacity of around 400 veh/h for the City center compared to Wiedikon is due to the City center's extensive public transport priority system (for more details, see Ortigosa et al. (2014)). Figure 2(b) shows the familiar relationship between average speed and density. In general, Wiedikon shows greater free flow speeds than the City center. We attribute this to the differences in intersection density

(see Table 1). Wiedikon has longer average links and less intersections than the denser City center, thus, vehicles in Wiedikon need to stop less frequently.

Similar to Chiabaut (2015), we compute the car passenger density by multiplying vehicle density by two-hour averages of car passenger occupancy. The latter value is calculated from the trip diary of the Swiss transportation micro-census 2010 (Swiss Federal Statistical Office (BFS), 2012). We select all car trips by drivers heading for any part of Zurich (including both the City center and Wiedikon) and compute the mean car occupancy for weekdays and two-hour intervals, e.g. one value for 06:00 to 08:00, one for 08:00 to 10:00, etc. This makes the calculations of the 3D-pMFD more accurate than taking one average value over the whole time period. Note, average car occupancy during the morning peak is around 1.2 and increases toward the evening to 1.36.

2.3 Public transport data

Data on public transport performance is obtained from Zurich's transit operator, *Verkehrsbetriebe Zürich* (VBZ). The data set contains information on each public transport vehicle's travel time from stop to stop, t_i , including the dwell time at each stop (Stadt Zürich, 2016b), recorded by automatic vehicle location (AVL) devices. We add the distance d_i from stop to stop, and compute the mean speed $v_{i,pt} = d_i/t_i$ (Leclercq et al., 2014). A unique vehicle identifier in the data set allows us to count the number of vehicles N_{pt} at any point in time within the defined regions.

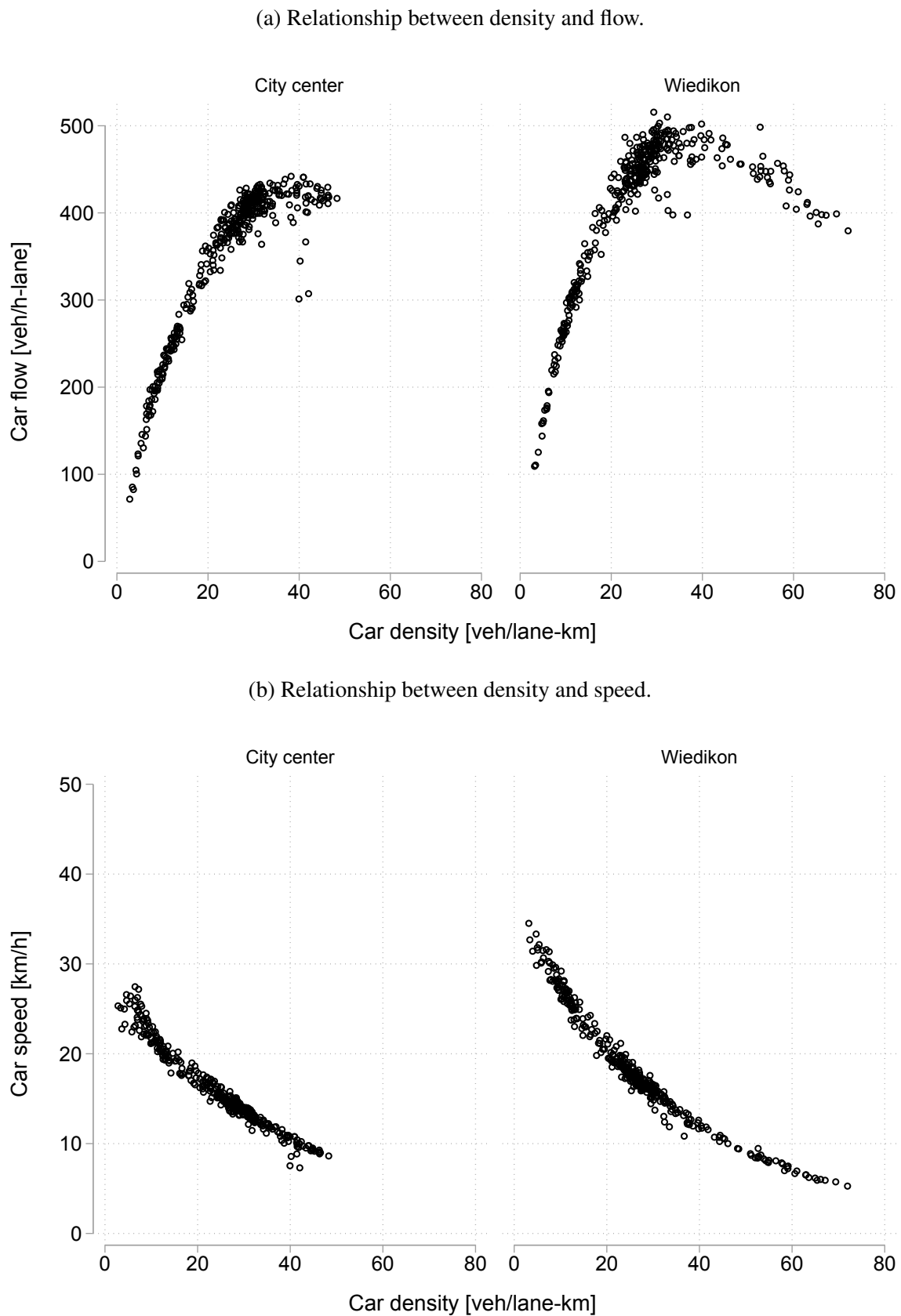
Vehicle occupancies are available for the year 2014 (Stadt Zürich, 2016a). This data set contains - for each line - type of day, scheduled trip, and leg between two stops, as well as the annual average passenger counts. We do not expect significant changes in occupancies between 2014 and 2015, given the absence of exogenous changes in the city and region. For each time interval, the average speed v_{pt} of public transport vehicles is computed according to Equation 4.

$$v_{pt} = \frac{\sum_{i=1}^N v_{i,pt} l_i}{\sum_{i=1}^N l_i} \quad (4)$$

The average density k_{pt} is computed with Equation 5 using a network length L_{pt} .

$$k_{pt} = \frac{N_{pt}}{L_{pt}} \quad (5)$$

Figure 2: Macroscopic relationships for the car traffic in Zurich.



Then we calculate public transport vehicle flow, q_{pt} with Equation 6.

$$q_{pt} = k_{pt}v_{pt} \quad (6)$$

3 Empirical 3D-MFD

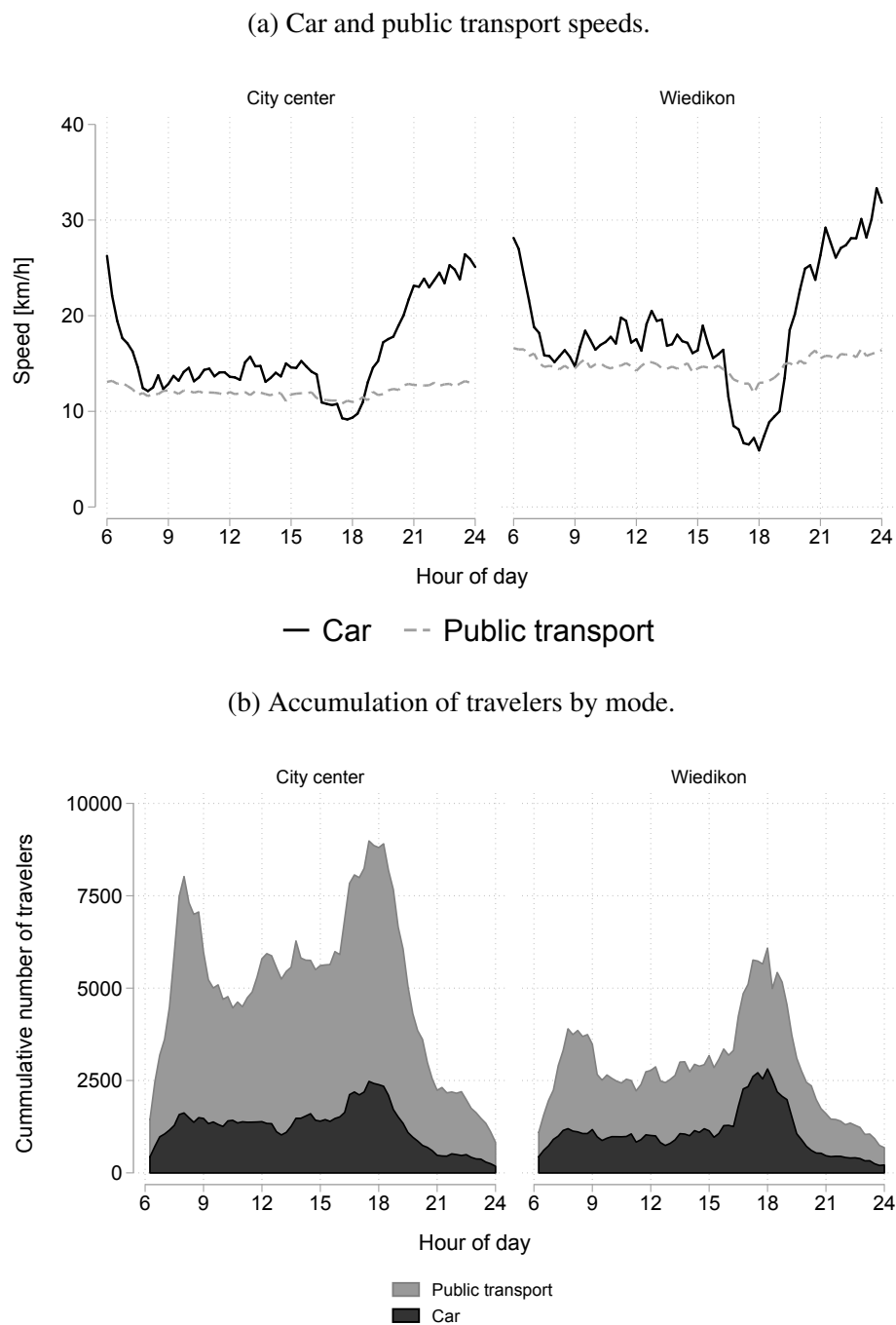
In this analysis, we focus on bi-modal interactions and their implications for speeds of the private and public modes. We aggregate all data points into 15 min intervals to avoid systematic variation in the 3D-MFD, due to the relatively rigid fixed-interval timetable for public transportation in Zurich.

In Figure 3(a) we compare the speeds of cars and public transport vehicles during Tuesday, October 27th 2015. Remember that the speeds of public transport vehicles contain the dwell times. In the City center, we observe that the car speeds decrease during the morning and afternoon peak and remain at around 14 to 15 km/h during the day. The speed of public transport vehicles is around 12 km/h all the time, but shows a slight decrease to around 10 km/h during the afternoon peak. In Wiedikon, speeds of both modes are higher than in the City center and show a greater variance. In the afternoon, car speeds drop remarkably below public transport speeds.

Figure 3(b) shows the total number of travelers in the two regions, staked by mode. We observe - for both regions - that travel demand increases significantly during morning and evening peaks. The increase in travel demand during peak hours in the City center is mostly captured by public transport, whereas in Wiedikon, both modes show a similar increase. Regarding the share of public transport users, we observe a higher share in the City center than Wiedikon. We attribute this to the higher concentration of public transport lines in the City center (see Table 1).

In Figure 4, we present the observed 3D-MFDs for the City center and Wiedikon. The horizontal plane represents the accumulation of both modes and the vertical axis the total vehicle flow. Since this is an empirical data set, the range of observed data points is limited, especially for public transport accumulation (due to tight timetables). That being said, we can still compare the two similarly-sized regions. In general, we register higher public transport accumulation for the City center than for Wiedikon, due to the very high number of public transport lines found in the City center. Conversely, slightly higher car accumulations are registered in Wiedikon than in the City center. For any given car accumulations, we observe a higher vehicle flow in Wiedikon than in the City center.

Figure 3: Bi-modal relationships in the city of Zurich.

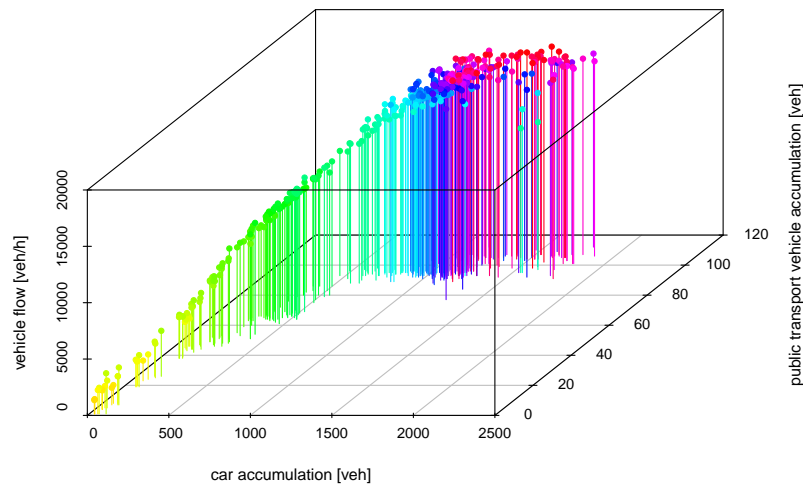


4 A statistical model for the 3D-MFD based on empirical data

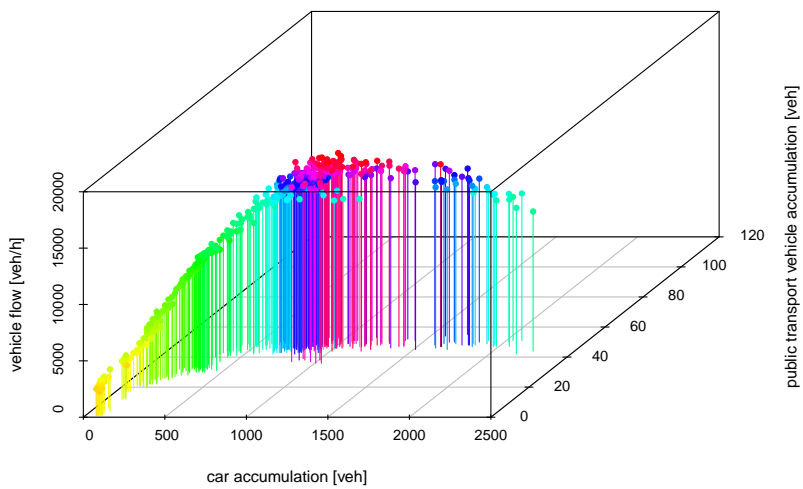
With the available - but limited - range of data, in this section, we quantify the macroscopic relationships using a statistical model. This allows us to use the 3D-MFD in further applications. Figure 4 shows trends similar to those found in Geroliminis et al. (2014) for the 3D-MFD using simulation data, but our data does not exhibit similar experimental variation because it is

Figure 4: 3D-MFDs in Zurich

(a) City center.



(b) Wiedikon.



empirical. Geroliminis et al. (2014) propose linking car and public transport density to total flow exponentially with a bivariate quadratic function of both modes' densities. However, with our data showing limited empirical variation, we cannot estimate this function, especially because extreme values must be arbitrarily defined to fit the curve. Therefore, we follow Zheng and Geroliminis (2016b), and define functions for the vehicle based 3D-MFD and the passenger 3D-MFD (3D-pMFD), based on observed data. Note that accumulation, n , can be easily transformed into density, if the network length, L_c or L_{pt} , is known, $k_c = n_c/L_c$ or $k_{pt} = n_{pt}/L_{pt}$. In the

following, we introduce a model based on densities, rather than accumulation, to normalize for the different regions

4.1 3D-MFD

For simplicity and as a first order approach, we model a linear relationship between density and speed (in accordance with Mahmassani et al. (1987)). The speed of public transport, v_{pt} , is modeled by a linear relationship for car speed \tilde{v}_c , as proposed by Geroliminis et al. (2014) and Zheng and Geroliminis (2013) and covers mode interactions.

Therefore, we propose modeling the 3D-MFD using empirical data using two equations. The first equation links car speeds \tilde{v}_c to free flow speed $\beta_{c,0}$, the density of cars \tilde{k}_c and the density of public transport vehicles k_{pt} . β_c and β_{pt} are coefficients to be estimated from the data and represent the marginal effect of each mode.

$$\tilde{v}_c = \beta_{c,0} + \beta_c \tilde{k}_c + \beta_{pt} k_{pt} \quad (7)$$

Using the definition by Geroliminis et al. (2014) and Zheng and Geroliminis (2013), the speed of public transport vehicles v_{pt} is defined in Equation 8 as a function of car speed \tilde{v}_c . Thus, public transport speed does not explicitly depend on vehicles' densities \tilde{k}_c and k_{pt} . However, \tilde{v}_c is a function of vehicle densities and therefore v_{pt} depends implicitly on vehicle densities. The coefficients to be estimated are $\beta_{pt,0}$ and $\beta_{c,pt}$. $\beta_{c,pt}$ captures the aspect that public transport vehicles typically move more slowly than cars due to frequent stops, and $\beta_{pt,0}$ adjusts for the fact that public transport speeds might exceed car speeds during congested time due to dedicated lanes. This effect is observed in both regions during the evening peak, see Figure 3(a).

$$v_{pt} = \beta_{c,pt} v_c + \beta_{pt,0} \stackrel{Eq.7}{=} \beta_{c,pt} (\beta_{c,0} + \beta_c \tilde{k}_c + \beta_{pt} k_{pt}) + \beta_{pt,0} \quad (8)$$

4.2 3D-pMFD

The 3D-pMFD is estimated by substituting vehicle densities in Equation 7 for passenger densities $\tilde{k}_{pax,c}$ for cars and $k_{pax,pt}$ for public transport, as introduced by Chiabaut (2015). Thus, the resulting model equation is changed to Equation 9. In this approach, Equation 8 for public

Table 2: Model estimates for the vehicle 3D-MFD. The dependent variables are the space-mean speeds of cars and public transport vehicles. All estimates are significant at 1 % level of significance.

	City center		Wiedikon	
	Car	Public transport	Car	Public transport
Car density [veh/km]	-0.355		-0.362	
Pub. tr. vehicle density [veh/km]	-1.223		-5.442	
Car speed [km/h]		0.125		0.121
Constant	27.935		37.503	
Constant		10.049		12.614
R^2	0.96	0.72	0.95	0.77
N	365	365	365	365

transport vehicle speeds still holds.

$$\tilde{v}_c = \beta_{pax,c,0} + \beta_{pax,c} \tilde{k}_{pax,c} + \beta_{pax,pt} k_{pax,pt} \quad (9)$$

5 Model results

5.1 3D-MFD

In Table 2, we show model estimates for the vehicle 3D-MFD for both regions in Zurich. All estimates are significant and show the expected sign. Wiedikon shows a higher free flow speed than the City center and a similar marginal effect of cars; both findings are in accordance with the results from Figure 2(b). The higher free flow speed can be attributed to longer links and fewer signalized intersections in Wiedikon (see Table 1). Comparing the marginal effects of public transport vehicles, we find -1.2 km/h per vehicle in the City center and -5.4 km/h per vehicle in Wiedikon. In addition, we compute the elasticities at mean of both vehicle densities on car speed. The elasticity in the City center is -0.2 and in Wiedikon -0.5. We expect that the lower impact of public transport vehicles in the City center is due to the larger share of dedicated lanes. Considering public transport speeds, we observe 12.6 km/h in Wiedikon and 10.0 km/h in the City center for the constant $\beta_{pt,0}$ and around 0.12 km/h per car speed change in km/h in both zones. Again, we also compute, the elasticity between car speed and public transport speed and find it to be around 0.15 for both regions. These findings are in line with Figure 3(a).

Table 3: Model estimates for the passenger 3D-MFD. The dependent variables are the space-mean speeds of cars and public transport vehicles. All estimates are significant at 1 % level of significance except those annotated otherwise.

	City center		Wiedikon	
	Car	Public transport	Car	Public transport
Car passenger density [pax/km]	-0.273		-0.225	
Pub. tr. passenger density [pax/km]	-0.005*		-0.067	
Car speed [km/h]		0.125		0.121
Constant	25.192		30.909	
Constant		10.049		12.614
R^2	0.92	0.72	0.89	0.77
N	360	365	360	365

* Not significant at 1 % level of significance but significant at 10 % level of significance.

5.2 3D-pMFD

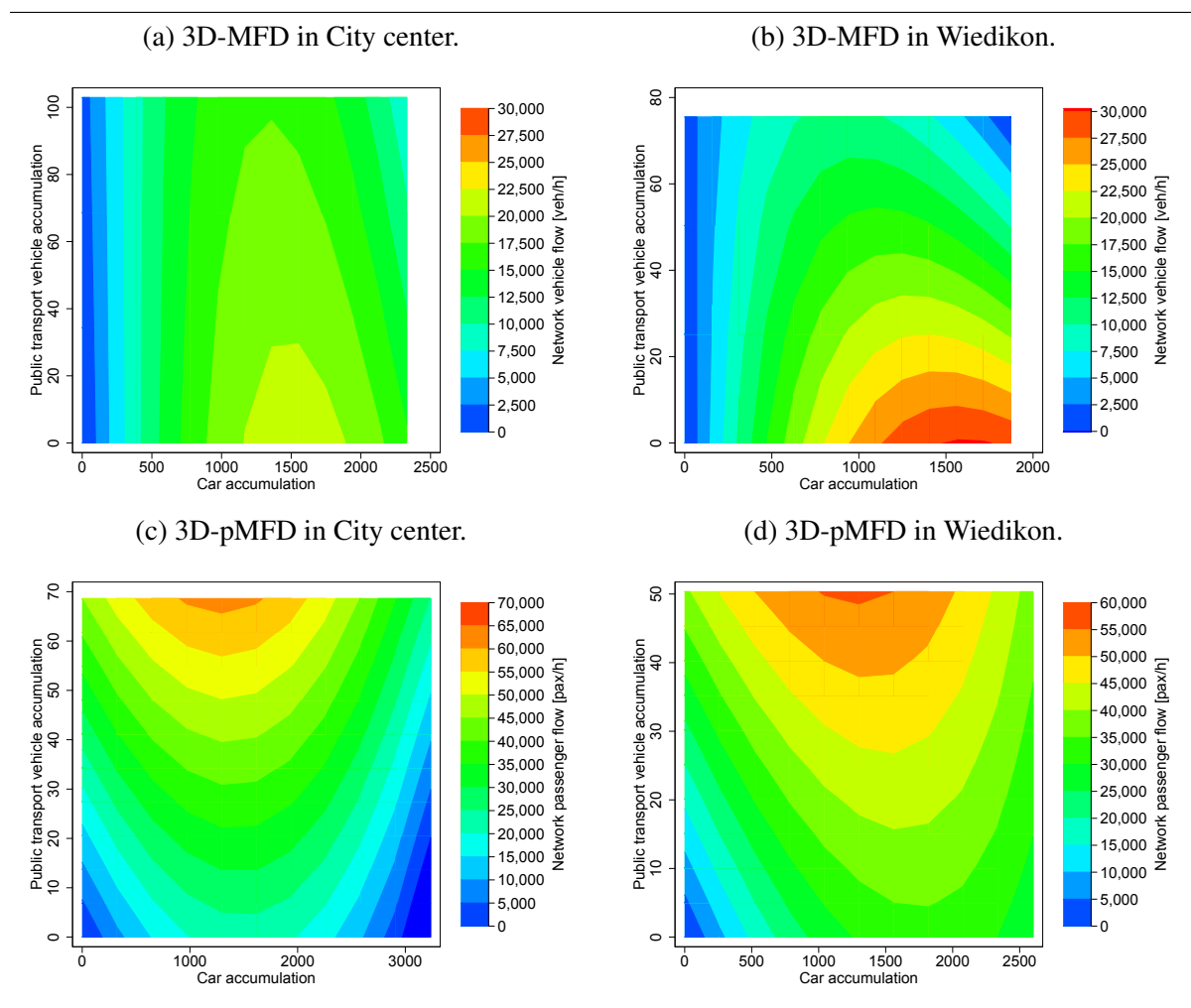
For the 3D-pMFD, Table 3 presents the model estimates. All model estimates show the expected sign and are significantly different from zero. Compared to the vehicle 3D-MFD estimates, differences in effect sizes of the 3D-pMFD reflect different vehicle occupancies. Note that estimates for public transport speed are identical because the model equation has not changed. The model estimates for the car speed equations emphasize that one additional passenger does, at least, impose one order of magnitude less impact on all car drivers when he chooses public transport instead of the car. In the City center, this ratio is even stronger than in Wiedikon, arguably, again, due to the larger share of dedicated lanes in the City center than in Wiedikon.

5.3 Predicted 3D-MFD

Using Table 2 we predict the familiar 3D-MFD shape (as introduced by Geroliminis et al. (2014)) for both regions in Figures 5(a) and 5(b). Speeds \hat{v}_c and \hat{v}_{pt} are calculated over a range of densities k_c and k_{pt} . Thus, we calculate the total network flow with $\hat{q}_{tot} = k_c \hat{v}_c L_c + k_{pt} \hat{v}_{pt} L_{pt}$. The 3D-pMFDs in Figures 5(c) and 5(d) are based on estimates from Table 3.

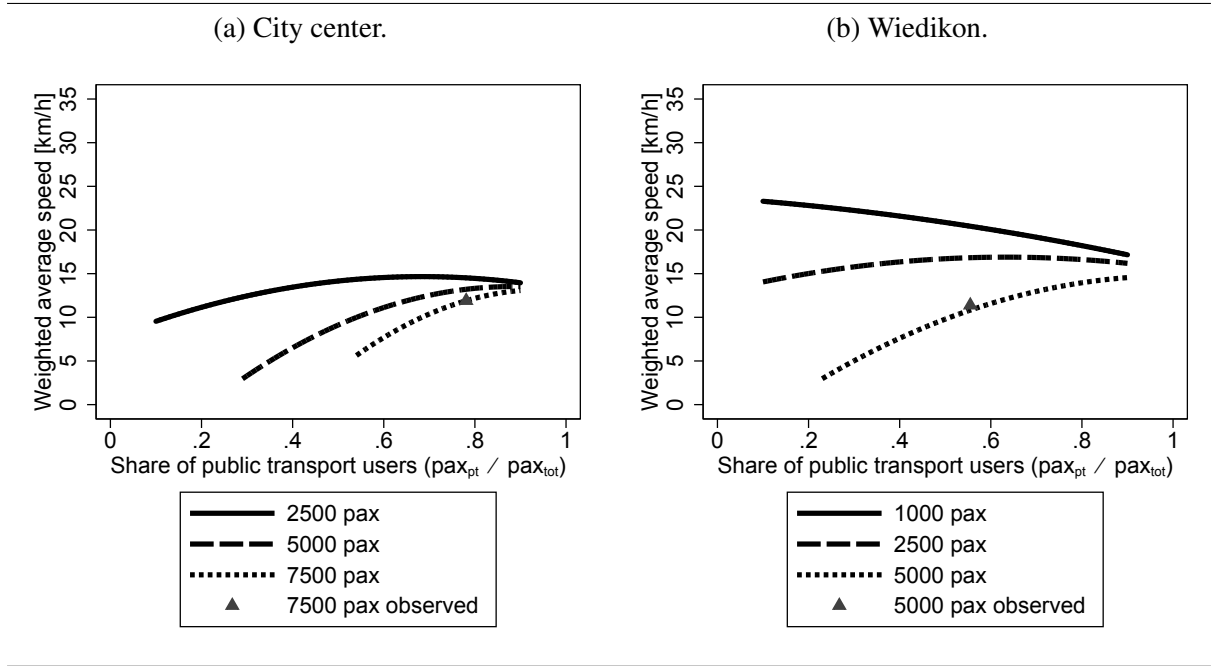
Arguably, the curves' shapes are mainly determined by the functional form of the model. However, the figures illustrate a plausible vehicle and passenger 3D-MFD. Maximum vehicle flow occurs at zero accumulation of public transport vehicles and, for a given car accumulation, increasing public transport accumulation reduces vehicular flow. In contrast, passenger flow increases with greater accumulation of public transport passengers, whereas the maximum

Figure 5: Predicted 3D-MFD shape for passenger and vehicles.



passenger flow is outside the range of observed accumulations. Interestingly, the maximum vehicle flow as a function of the public transport accumulation exhibits different behavior for the City center than for Wiedikon. The maximum vehicle flow for any given public transport accumulation is found at around 1500 cars. However, for Wiedikon, the maximum vehicle flow changes with the public transport vehicles. This confirms that the interaction between cars and public transport is higher in Wiedikon than in the City center - particularly due to the different share of dedicated lanes.

Figure 6: Share of public transport passengers and average journey speeds in Zurich.



6 Optimal share of public transport users based on the 3D-pMFD

An interesting application of the 3D-MFD is to compute and compare journey speeds of car users v_c and public transport users v_{pt} of a given population of travelers (excluding users's access time) (Wardrop, 1968; Mogridge, 1997). We define weighted average journey speed \bar{v} of car passengers pax_c and public transport passengers pax_{pt} in Equation 10 as a function of total travel demand $pax_{tot} = pax_c + pax_{pt}$ and share of public transport users pax_{pt}/pax_{tot} .

$$\bar{v} = \frac{v_{pt}pax_{pt} + v_cpax_c}{pax_{tot}} \quad (10)$$

This can be seen as a supply function of infrastructure's capacity, i.e. which travel times can be reached given a certain infrastructure. We use the passenger 3D-MFD for both regions and compute the weighted average journey speed as a function of share of public transport users for three demand levels indicated in Figure 6. The share of public transport users maximizing weighted average journey speed can be seen as an *optimal share* from the infrastructure capacity perspective. Note that we only plot realistic optimal shares (0.1-0.9). We observe a similar pattern in both regions; when the number of passengers increases, a larger number must use public transport to maximize the weighted average journey speed. Not surprisingly, the region of Wiedikon provides higher average speeds for the same combination of travel demand.

Furthermore, we analyzed empirical data for passenger levels around $pac_{tot} = 7500$ in the City center and $pac_{tot} = 5000$ in Wiedikon; both values represent the average number of passengers during peak hours. These observed values are shown as a triangle in Figure 6. They give an insight on how well existing demand is distributed across respective modes. We see that the City center already has a high share of public transport users, which leads to a speed close to the optimum. On the other side, Wiedikon would benefit from a higher share of public transport users during peak hours.

7 Conclusions

This paper presents the first empirical 3D-MFD for vehicles and passengers, in two regions in Zurich. The 3D-MFDs are estimated based on loop detector data, GPS trajectories of public transport vehicles, and vehicle occupancies (i.e., number of passengers per vehicle). We use a linear model between the accumulation of vehicles and car speeds and a linear model between public transport and car speeds. We observe a negative marginal effect for both public transport and cars, in line with previous studies (Smeed, 1961, 1968; Geroliminis et al., 2014). The marginal effect of one public transport vehicle is 3 to 10 times greater than the marginal effect of a car. The elasticity of public transport vehicles on car speeds in the City center is -0.23 and in Wiedikon -0.52 . We attribute these significant differences in the two regions to the higher share of dedicated public transport lanes in the City center. Even though both regions already have high shares of dedicated lanes for public transport, it is important to note that other, substantial interactions are present, especially at intersections. This effect is amplified in Zurich, since the public transport prioritization scheme in Zurich gives high priority to public transport (Ambühl et al., 2017).

We introduce a novel application of the 3D-pMFD, discussing an optimal share of public transport users. We emphasize that starting from a certain level of travel demand, the provision of public transport is necessary to improve urban speeds. With the 3D-MFD, policy makers and transport planners can assess policy changes at vehicle and passenger level for both modes. In essence, a comparison between the observed and the optimal share of public transport users gives quantitative insights on how efficiently a city's multimodal transportation network operates. Authorities can then formulate changes necessary to shift the network to its optimum directly from a 3D-pMFD. Recall that the policy-relevant implications should be carefully evaluated because of limited variance and range in the data. However, most applications building on - and around - the 3D-MFD and the 3D-pMFD will be based on the observed equilibrium. For such small deviations around the observed 3D-MFD, our estimates are appropriate.

This study does have some data limitations. Overall, the limited exogenous empirical variation in public transport due to tight timetables limits the validity of model estimates to the observed range and does not allow estimation of second order effects. Complete car data is not available for all links and public transport provision is not homogeneously distributed on the entire road network. This implies that our 3D-MFD might be biased due to an unrepresentative sample, but as the covered network length is large, we expect this bias to be small. We aggregated the sample at 15 min intervals to avoid random scattering caused by the public transport timetable when considering smaller intervals. These greater intervals, in turn, reduce the sample size for model estimation. As the timetable and public transport vehicles' routes cannot be changed 'ad libitum', a homogeneous distribution of public transport vehicles in space and time using smaller intervals is not possible.

Our future research will concentrate on analytical approximations of the 3D-MFD following the work by Daganzo and Geroliminis (2008), Chiabaut (2015), Boyac and Geroliminis (2011), Leclercq and Geroliminis (2013) and Geroliminis and Boyacı (2012). This kind of work would not only improve general understanding of the 3D-MFD, but would also allow derivation of a methodology to estimate the 3D-MFD with less data, based on infrastructure and public transport system parameters.

8 Acknowledgments

This work was supported by ETH Research Grants ETH-04 15-1 and ETH-27 16-1. We would like to thank the City of Zurich for providing loop detector data and public transport data.

9 References

- Aboudolas, K. and N. Geroliminis (2013) Perimeter and boundary flow control in multi-reservoir heterogeneous networks, *Transportation Research Part B: Methodological*, **55**, 265–281.
- Adler, M. W. and J. N. van Ommeren (2016) Does public transit reduce car travel externalities? Quasi-natural experiments' evidence from transit strikes, *Journal of Urban Economics*, **92**, 106–119.
- AKP Verkehrsingenieure AG (2016) Forschungsprojekt VSS 2011/203 Geometrie des Fahrzeugparks der Schweiz.

- Ambühl, L., A. Loder, M. Menendez and K. W. Axhausen (2017) Empirical macroscopic fundamental diagrams: New insights from loop detector and floating car data. . Accepted for presentation at TRB 96th Annual Meeting.
- Ambühl, L. and M. Menendez (2016) Data fusion algorithm for macroscopic fundamental diagram estimation, *Transportation Research Part C: Emerging Technologies*, **71**, 184–197.
- Anderhub, G., R. Dorbritz and U. Weidmann (2008) Leistungsfähigkeitsbestimmung öffentlicher Verkehrssysteme, *Schriftenreihe*, **139**, IVT, ETH Zurich, Zurich.
- Anderson, M. L. (2014) Subways, strikes, and slowdowns: The impacts of public transit on traffic congestion, *The American Economic Review*, **104** (9) 2763–2796.
- Arnet, K., S. I. Guler and M. Menendez (2015) Effects of Multimodal Operations on Urban Roadways, *Transportation Research Record*, **2533**, 1–7, nov 2015.
- Boyac, B. and N. Geroliminis (2011) Estimation of the network capacity for multimodal urban systems, *Procedia - Social and Behavioral Sciences*, **16**, 803 – 813.
- Buisson, C. and C. Ladier (2009) Exploring the Impact of Homogeneity of Traffic Measurements on the Existence of Macroscopic Fundamental Diagrams, *Transportation Research Record: Journal of the Transportation Research Board*, **2124**, 127–136.
- Cao, J. and M. Menendez (2015) System dynamics of urban traffic based on its parking-related-states, *Transportation Research Part B: Methodological*, **81**, 718–736.
- Chatman, D. G. and R. B. Noland (2011) Do public transport improvements increase agglomeration economies? a review of literature and an agenda for research, *Transport Reviews*, **31** (6) 725–742.
- Chiabaut, N. (2015) Evaluation of a multimodal urban arterial: The passenger macroscopic fundamental diagram, *Transportation Research Part B: Methodological*, **81**, Part 2, 410 – 420.
- Chiabaut, N., X. Xie and L. Leclercq (2016) Performance analysis for different designs of a multimodal urban arterial, *Transportmetrica B: Transport Dynamics*, **2** (3) 229–245.
- Christofa, E., K. Ampountolas and A. Skabardonis (2016) Arterial traffic signal optimization: a person-based approach, *Transportation Research Part C: Emerging Technologies*, **66**, 27–47.
- Courbon, T. and L. Leclercq (2011) Cross-comparison of macroscopic fundamental diagram estimation methods, *Procedia-Social and Behavioral Sciences*, **20**, 417–426.

- Daganzo, C. F. and N. Geroliminis (2008) An analytical approximation for the macroscopic fundamental diagram of urban traffic, *Transportation Research Part B: Methodological*, **42** (9) 771–781.
- Du, J., H. Rakha and V. V. Gayah (2016) Deriving macroscopic fundamental diagrams from probe data: Issues and proposed solutions, *Transportation Research Part C: Emerging Technologies*, **66**, 136–149.
- Geroliminis, N. (2015) Cruising-for-parking in congested cities with an mfd representation, *Economics of Transportation*, **4** (3) 156–165.
- Geroliminis, N. and B. Boyacı (2012) The effect of variability of urban systems characteristics in the network capacity, *Transportation Research Part B: Methodological*, **46** (10) 1607–1623.
- Geroliminis, N. and C. F. Daganzo (2008) Existence of urban-scale macroscopic fundamental diagrams: Some experimental findings, *Transportation Research Part B: Methodological*, **42** (9) 759–770.
- Geroliminis, N., N. Zheng and K. Ampountolas (2014) A three-dimensional macroscopic fundamental diagram for mixed bi-modal urban networks, *Transportation Research Part C: Emerging Technologies*, **42**, 168 – 181.
- Godfrey, J. W. (1969) The Mechanism of a Road Network, *Traffic Engineering and Control*, **11** (7) 323–327.
- Gronau, R. (2000) Optimum diversity in the public transport market, *Journal of Transport Economics and Policy*, **34** (1) 21–41.
- Haddad, J. and N. Geroliminis (2012) On the stability of traffic perimeter control in two-region urban cities, *Transportation Research Part B: Methodological*, **46** (9) 1159–1176.
- Hensher, D. A. (2001) Measurement of the valuation of travel time savings, *Journal of Transport Economics and Policy*, **35** (1) 71–98.
- Ji, Y., J. Luo and N. Geroliminis (2014) Empirical observations of congestion propagation and dynamic partitioning with probe data for large-scale systems, *Transportation Research Record: Journal of the Transportation Research Board*, **2422**, 1–11.
- Knoop, V. L., D. de Jong and S. Hoogendoorn (2014) The influence of the road layout on the Network Fundamental Diagram, *TRB 93rd Annual Meeting Compendium of Papers*, 1–16.
- Knoop, V. L., H. van Lint and S. P. Hoogendoorn (2015) Traffic dynamics: Its impact on the Macroscopic Fundamental Diagram, *Physica A: Statistical Mechanics and its Applications*, **438**, 236–250.

- Köhler, U., S. Strauss and S. Wichmann (1998) *Berichte der Bundesanstalt für Strassenwesen. Verkehrstechnik*, **57**, Wirtschaftsverlang NW, Bremerhaven.
- Leclercq, L., N. Chiabaut and B. B. Trinquier (2014) Macroscopic Fundamental Diagrams: A cross-comparison of estimation methods, *Transportation Research Part B: Methodological*, **62**, 1–12.
- Leclercq, L. and N. Geroliminis (2013) Estimating mfd in simple networks with route choice, *Transportation Research Part B: Methodological*, **57**, 468–484.
- Lüthy, N., S. I. Guler and M. Menendez (2016) Systemwide effects of bus stops: Bus bays vs. curbside bus stops, paper presented at the *TRB 95th Annual Meeting Compendium of Papers*, Washington, DC.
- Mahmassani, H., J. C. Williams and R. Herman (1984) Investigation of network-level traffic flow relationships: some simulation results, *Transportation Research Record: Journal of the Transportation Research Board*, **971**, 121–130.
- Mahmassani, H., J. C. Williams and R. Herman (1987) Performance of urban traffic networks, in N. Gartner and N. H. M. Wilson (eds.) *Proceedings of the 10th International Symposium on Transportation and Traffic Theory*, 1–20, Elsevier Science Publishing.
- Menendez, M., J. Ortigosa, L. Ambühl, K. W. Axhausen, F. Ciari, P. M. Bösch, N. Geroliminis and N. Zheng (2016) NetCap: Intermodale Strecken- /Linien- und Netzleistungsfähigkeit, Schlussbericht SVI 2004/032, *Schriftenreihe*, **1563**, IVT ETH Zürich und LUTS EPF Lausanne.
- Mogridge, M. J. H. (1997) The self-defeating nature of urban road capacity policy: A review of theories, disputes and available evidence, *Transport Policy*, **4** (1) 5–23.
- Muhlich, N., V. V. Gayah and M. Menendez (2015) An Examination of MFD Hysteresis Patterns for Hierarchical Urban Street Networks Using Micro-Simulation, *Transportation Research Record: Journal of the Transportation Research Board*, **2491**, 117–126, oct 2015.
- Open Street Map (2016) Downloaded with R's ggmap package.
- Ortigosa, J., M. Menendez and V. V. Gayah (2015) Analysis of Network Exit Functions for Various Urban Grid Network Configurations, *Transportation Research Record: Journal of the Transportation Research Board*, **2491**, 12–21.
- Ortigosa, J., M. Menendez and H. Tapia (2014) Study on the number and location of measurement points for an MFD perimeter control scheme: a case study of Zurich, *EURO Journal on Transportation and Logistics*, **3** (3-4) 245–266.

- Ortigosa, J., N. Zheng, M. Menendez and N. Geroliminis (2017) Analysis of the 3D-vMFDs of the urban networks of Zurich and San Francisco. . Accepted for presentation at TRB 96th Annual Meeting.
- Schreiber, A., A. Loder and K. W. Axhausen (2016) Urban mode and subscription choice - An application of the three-dimensional MFD, *paper presented at the 16th Swiss Transport Research Conference, Ascona, May 2016*.
- Small, K. A. and E. T. Verhoef (2007) *The Economics of Urban Transportation*, Routledge, Abingdon.
- Smeed, R. J. (1961) *The traffic problem in towns*, Statistical Society, Manchester.
- Smeed, R. J. (1968) Traffic Studies and Urban Congestion, *Journal of Transport Economics and Policy*, **2** (1) 33–70.
- Stadt Zürich (2016a) Fahrgastzahlen VBZ, Stadt Zürich Open Data, <https://data.stadt-zuerich.ch/dataset/vbz-fahrgastzahlen-ogd>.
- Stadt Zürich (2016b) Fahrzeiten der VBZ im Soll-Ist-Vergleich, Stadt Zürich Open Data, <https://data.stadt-zuerich.ch/dataset/vbz-fahrzeiten-ogd>.
- Stadt Zürich - Dienstabteilung Verkehr (DAV) (2015) Loop detector data in Zurich.
- Swiss Federal Statistical Office (BFS) (2012) *Mobilität in der Schweiz - Ergebnisse des Mikrozensus Mobilität und Verkehr 2010*, Swiss Federal Statistical Office (BFS), Neuchatel.
- Thomson, J. (1967) Speeds and flows of traffic in central london: 2. speed-flow relations, *Traffic Engineering & Control*, **8** (12) 721–725.
- Tirachini, A. and D. A. Hensher (2012) Multimodal transport pricing: First best, second best and extensions to non-motorized transport, *Transport Reviews*, **32** (2) 181–202.
- Tsubota, T., A. Bhaskar and E. Chung (2014) Macroscopic fundamental diagram for Brisbane, Australia: empirical findings on network partitioning and incident detection, *Transportation Research Record: Journal of the Transportation Research Board*, **2421**, 12–21.
- Vasileios, N., S. I. Guler and M. Menendez (2016) Effects of bus operations on the traffic capacity of urban networks: A simulation study, paper presented at the *Transportation Research Board 95th Annual Meeting*.
- Wang, P. F., K. Wada, T. Akamatsu and Y. Hara (2015) An empirical analysis of macroscopic fundamental diagrams for sendai road networks, *Interdisciplinary Information Sciences*, **21** (1) 49–61.

- Wardrop, J. (1968) Journey speed and flow in central urban areas, *Traffic Engineering & Control*, **9** (11) 528–532.
- Williams, J. C., H. S. Mahmassani, S. Iani and R. Herman (1987) Urban traffic network flow models, *Transportation Research Record: Journal of the Transportation Research Board*, **1112**, 78–88.
- Zheng, N. and N. Geroliminis (2013) On the distribution of urban road space for multimodal congested networks, *Transportation Research Part B: Methodological*, **57**, 326 – 341.
- Zheng, N. and N. Geroliminis (2016a) Modeling and optimization of multimodal urban networks with limited parking and dynamic pricing, *Transportation Research Part B: Methodological*, **83**, 36–58.
- Zheng, N. and N. Geroliminis (2016b) Modeling and optimization of multimodal urban networks with limited parking and dynamic pricing, *Transportation Research Part B: Methodological*, **83**, 36 – 58.
- Zheng, N., G. Rérat and N. Geroliminis (2016) Time-dependent area-based pricing for multimodal systems with heterogeneous users in an agent-based environment, *Transportation Research Part C: Emerging Technologies*, **62**, 133–148.
- Zheng, Y., R. A. Waraich, N. Geroliminis and K. W. Axhausen (2012) A dynamic cordon pricing scheme combining a macroscopic and an agent-based traffic model, *Transportation Research A*, **46** (8) 1291–1303.